

## **Chiral glutamic acid functionalized graphene: Preparation and application**

Qian Han<sup>a,b</sup>, Qiao Xia<sup>a</sup>, Dongmei Guo<sup>a</sup>, Can Li<sup>b</sup>, Yingzi Fu<sup>a\*</sup>

<sup>a</sup>Key Laboratory on Luminescence and Real-Time Analysis, Ministry of Education,  
College of Chemistry and Chemical Engineering, Southwest University, Chongqing  
400715, PR China

<sup>b</sup> Laboratory of Environment change and Ecological Construction of Hebei  
Province, College of Resources and Environment Science, Hebei Normal University,  
Shijiazhuang, Hebei 050024, PR China.

## **(Supplementary Material)**

### **EXPERIMENTAL SECTION**

**Reagents and Materials** Graphene oxide was obtained from Nan-jing xianfeng nano Co. (Nanjing, China), L- or D-3,4-dihydroxyphenylalanine (L- or D-DOPA, 99%), L- or D-glutamic acid (L- or D-Glu, >99%) were obtained from Sigma Chemical Co. (St. Louis, MO, USA). KOH, NaBH<sub>4</sub> were purchased from Chemical Reagent Co. (Chongqing, China). K<sub>3</sub>[Fe(CN)<sub>6</sub>], K<sub>4</sub>[Fe(CN)<sub>6</sub>], H<sub>2</sub>SO<sub>4</sub> and other chemicals were analytical grade and without further purification. Double distilled water was used throughout all experiments.

**Apparatus** All electrochemical measurements were performed with a CHI660A electrochemistry workstation (Shanghai Chenhua Instruments Co., China). Infrared spectra (IR) were collected with a Fourier-transform infrared spectrophotometer (GX, Perkin Elmer Co., USA) using KBr disks. UV-vis absorption spectra were recorded by a UV-8500 spectrometer (Shanghai Tianmei, China). The scanning electron micrograph was taken with scanning electron microscope (SEM, S-4800, Hitachi). A three-electrode cell equipped with a modified glassy carbon electrode (GCE,  $\phi = 4$  mm) as working electrode and a platinum wire was used as auxiliary electrode, a saturated calomel electrode (SCE) was as a reference electrode.

**Characterization of the materials by color change:** The reduction of graphene oxides was indicated from the color change of solution before and after reaction (from brown to dark, see Figure S1 a to c). Figure S1 indicated that the dispersions of the LGO and DGO in aqueous solution at concentrations of 0.5mg.ml<sup>-1</sup>. Compared with GO solution, the resulting LGO and DGO aqueous solution are very stable without

precipitation even after 24 h standing in an ambient environment.

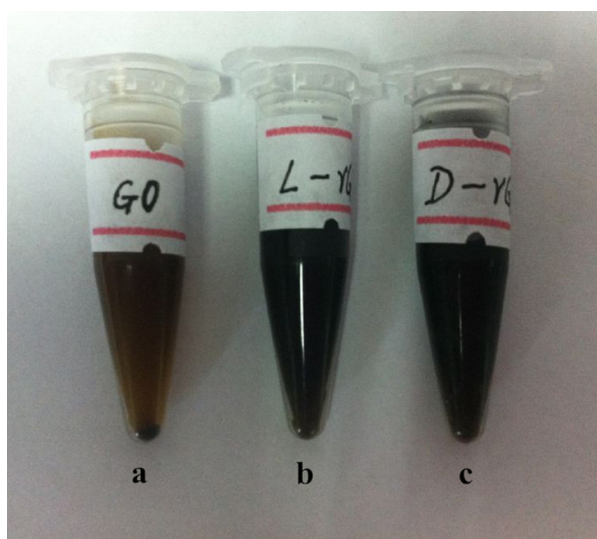


**Figure S1** Photos of (a) GO, (b) LGO and (c) DGO aqueous solution.

**Optimization of synthetic conditions.** The ratio of GO/L-Glu, pH and the temperature all affect the preparation of hybrids. UV-Vis absorption spectroscopy was used to monitor the effect of these factors on the reduction process (Figure S2). Take the LGO as an example, the amount of L-Glu was investigated (Fig.S 2a, pH=9.90). When the GO/L-Glu ratio was decreased continually,  $\lambda_{\max}$  shifted to a higher wavelength and reached 280nm. When the ratio of GO/L-Glu (w/w) was lower than 1:4,  $\lambda_{\max}$  shifted little. Considering a sufficient reaction, the ratio of L-Glu and GO was 1:4. The pH value has a significant influence on the synthetic materials (Fig.S 2b). The alkaline conditions were favorable for ring-opening reaction of epoxide and amine hydrogen. The pH effect of the solution was studied from pH 8.0 to 14.0. It showed that the absorption peak shifted to 280nm at pH 13.0 and the increasing pH value could not cause a further change in  $\lambda_{\max}$ . Hence, the solution pH of 13.0 was selected in the synthesis experiment. The effect of the temperature on the chiral hybrid was also investigated (Fig.S 2c). When the GO reduction was carried out at 50

and 60 °C, the  $\lambda_{\text{max}}$  only shifted to 245 and 261nm, respectively. When the reaction temperature was increased from 65 to 80 °C, the  $\lambda_{\text{max}}$  shifted to 280 nm, and the further increasing temperature could not cause obvious shift. Thus, 70 °C was chosen as the optimal reaction temperature.

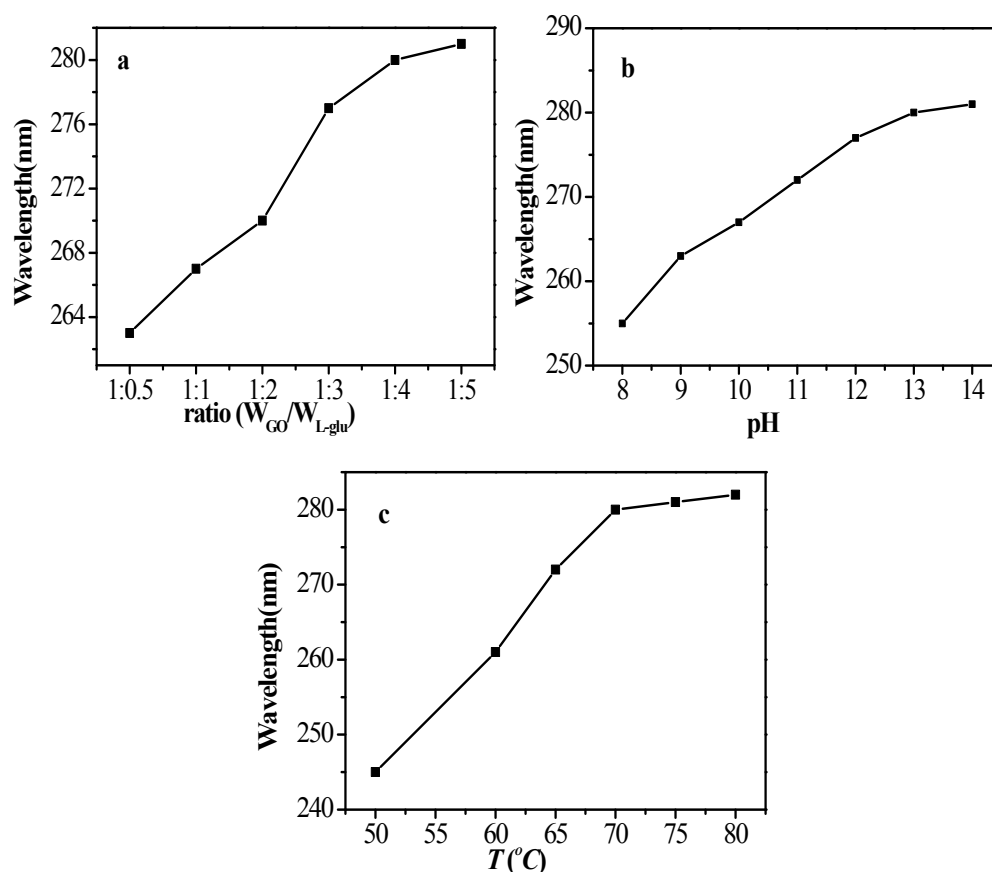
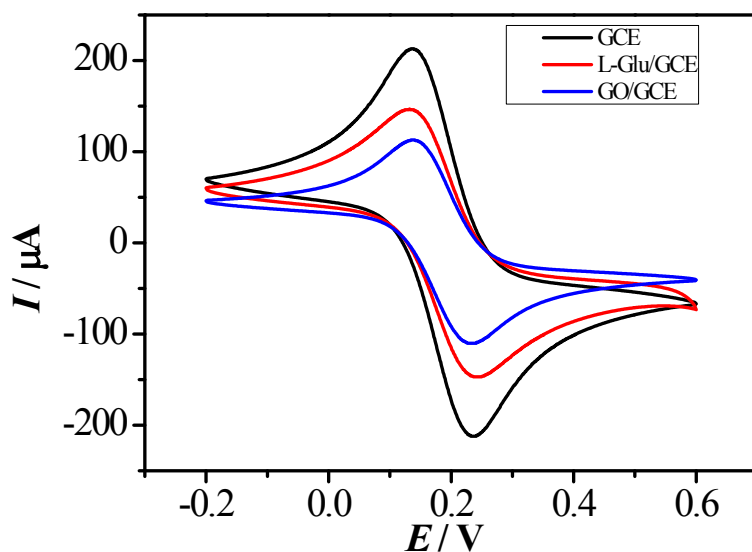


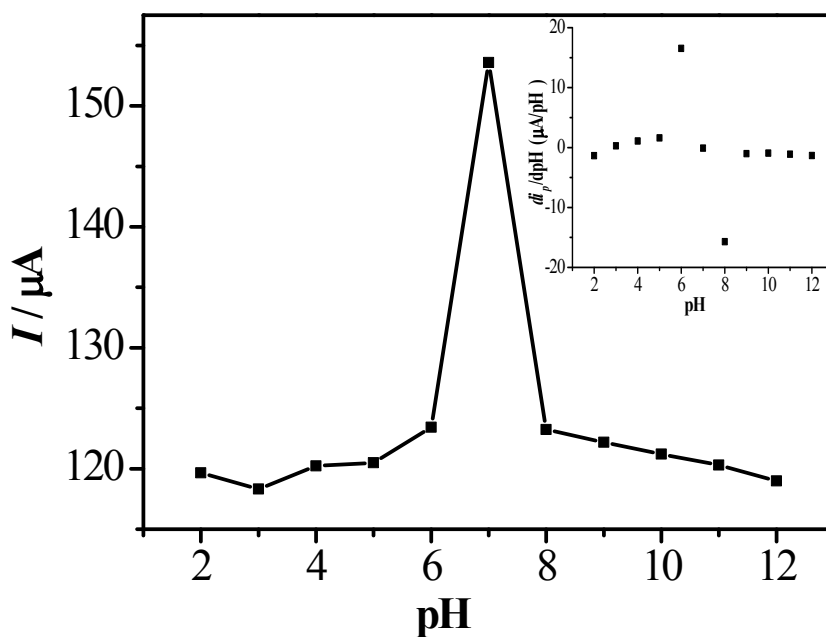
**Figure S2** The effect of (a) the ratio of GO/L-glu, (b) pH and (c) reaction temperature.

**Electrochemical characterization of the electrode surface.** The fabrication of the modified electrode was characterized by CV. As shown in FigureS3, the bare GCE showed a standard redox peak in 5 mM  $[\text{Fe}(\text{CN})_6]^{4-/3-}$  solution containing 0.1 M KCl. A decrease of peak current was observed after the L-Glu-graphene hybrid was dropped on the electrode (LGO/GCE). But the current peak was largely decreased on graphene oxide modified electrode (GO/GCE).



**FigureS3.** CVs of bare GCE (black line); L-Glu/GCE (red line); (c) GO/GCE (blue line) in the electrolyte containing 5 mM  $[\text{Fe}(\text{CN})_6]^{4-/3-}$  solution.

**Determination of surface pKa.** The surface pKa can be determined from the current parameter of CVs in  $[\text{Fe}(\text{CN})_6]^{4-/3-}$  solution of different pH. As we known, the redox current of  $[\text{Fe}(\text{CN})_6]^{4-/3-}$  is dependent on the pH of bulk solutions. Thus the current is conveniently used to investigate the dissociation of the end group of the L-glutamic acid graphene hybrid in different pH solutions. Figure S4 shows the dependence of the peak current on pH value (squares). The surface  $\text{pKa}_1$  was  $6.00 \pm 0.01$  and  $\text{pKa}_2$  was  $8.00 \pm 0.01$  from the peak of the differential curve (dots line) of the experimental data.



**FigureS4.** The relationship between pH and peak current; inset dots represents differential curve of experimental data.

**Influence of scan rate.** The influence of scan rate on the electro-oxidation of each enantiomeric of DOPA was studied by CV. As shown in FigureS5, the redox peak current increased with the scan rates in the range from 50 to 200  $\text{mV}\cdot\text{s}^{-1}$ , the peak current density and the square root of potential scan rate present a linear relationship, suggesting a diffusion confined process. The linear regression equation of LGO/GCE to D-DOPA was expressed as  $I_p (\mu\text{A}) = 30.68 v^{1/2} - 47.45$  ( $R=0.9747$ ), and the LGO/GCE to L-DOPA was expressed as  $I_p (\mu\text{A}) = 26.85v^{1/2} - 48.73$  ( $R = 0.9767$ ). These results further showed that the LGO/GCE had a high enantioselectivity to DOPA enantiomers.

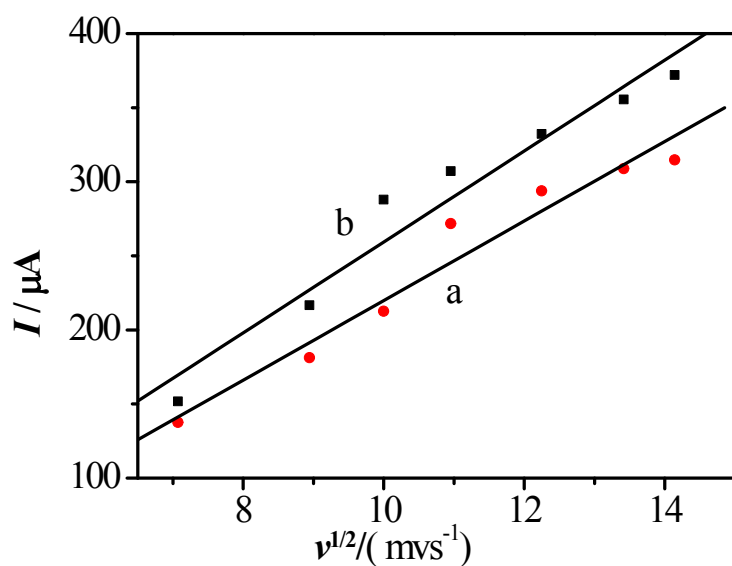


**Figure S5** The effect of the square root of potential sweep rate on LGO/GCE for (a) L-DOPA and (b) D-DOPA in 0.25 M H<sub>2</sub>SO<sub>4</sub>.

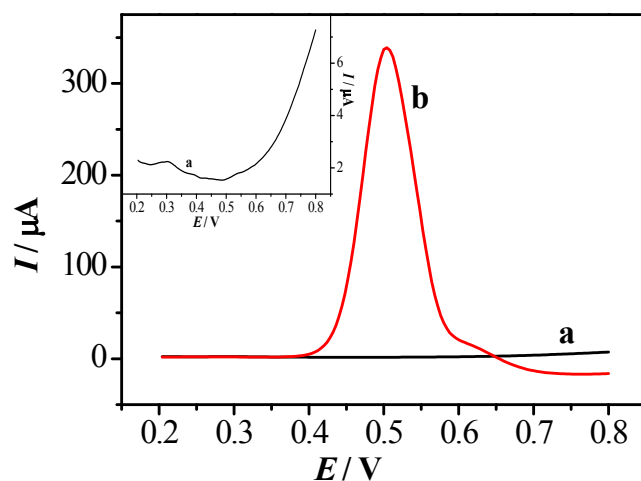
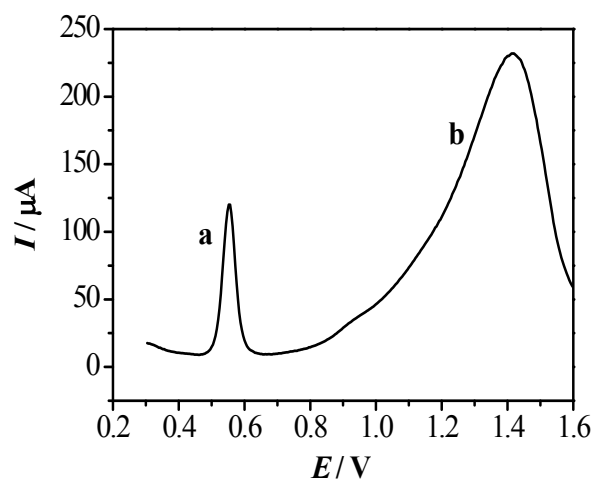


**Figure S6** The DNPV of LGO/GCE in the absence (curve a, black line) and in the presence of 5 mM L-DOPA (curve b, red line) in 0.25 M H<sub>2</sub>SO<sub>4</sub> solution.

**Interferences.** The interference of the 0.25 M H<sub>2</sub>SO<sub>4</sub> on LGO/GCE has been investigated (Figure S 6). The peak current of DOPA is much larger than the

background current, so background interference maybe negligible.



**FigureS 7** The effect of the 5-fold excess of AA on the determination of L-DOPA .

The DNPV was used to investigate the presence of AA on the behavior of 2mM D-DOPA (FigureS7). The AA signal was visible at about 1.41V, the presence of 5-fold excess of AA did not interference the response of DOPA at 0.552V.